Chemical Engineering Journal 98 (2004) 265–273

Chemical Engineering Journal

www.elsevier.com/locate/cej

Absorption of dilute SO_2 gas stream with conversion to polymeric ferric sulfate for use in water treatment

Aron D. Butler [a], Maohong Fan [a,*], Robert C. Brown [a], Adrienne T. Cooper [b], J.H. van Leeuwen [c], Shihwu Sung [c]

[a] *Center for Sustainable Environmental Technologies, Iowa State University, Ames, IA 50011, USA*
[b] *Department of Civil and Environmental Engineering, University of South Carolina, Columbia, SC 29208, USA*
[c] *Department of Civil, Construction and Environmental Engineering, Iowa State University, Ames, IA 50011, USA*

Accepted 13 October 2003

Abstract

Use of sulfur dioxide (SO_2) in the production of polymeric ferric sulfate (PFS) was investigated. PFS is a highly effective coagulant useful in treatment of drinking water and wastewater, and could serve as a value-added sink for sulfur removed during coal gas cleanup. SO_2 was absorbed from a dilute gas stream by sparging it into a bench-scale reactor containing a stirred solution of ferrous sulfate with sodium chlorate added as an oxidant. The reaction took place near atmospheric pressure and at temperatures of 30–80 °C, and produced a solution containing approximately 50 wt.% PFS. SO_2 removal efficiencies greater than 90% were achieved with ferrous iron concentrations in the product less than 0.1%. Other PFS quality parameters were also monitored, including total iron content, basicity, and pH. A factorial analysis of the effect of temperature, oxidant dosage, SO_2 concentration, and gas flow rate on SO_2 removal efficiency is presented. In general, higher synthesis temperatures increased iron conversion rates while decreasing SO_2 removal efficiency, and increased oxidant dosages had a positive correlation with removal efficiency. In addition, X-ray diffraction analyses showed that all dried PFS samples were found to be highly amorphous regardless of drying conditions.

Keywords: Sulfur dioxide; SO_2; Polymeric ferric sulfate; Fuel gas; Water treatment; Wastewater treatment

1. Introduction

Industrial ecology describes a system for achieving sustainability in human industrial endeavors, borrowing principles from natural ecosystems to optimize flows of materials and energy between processes, industries, and communities. It is a compelling solution because it provides economic incentives to reduce the adverse environmental impacts of industrial production processes [1].

Industrial ecology will be the framework for design for the next generation of fossil fuel electrical power plants. In these facilities coal will be gasified, allowing for processing of the fuel gas stream to remove sulfur and other pollutants prior to combustion, as well as production of a variety of other by-product gas and liquid streams that can be used as chemical feedstocks in other processes. Typical desulfurization processes involve calcium sorbents [2–4] where by-products are either of relatively low value, such as gypsum, or they are waste products requiring storage and eventual landfilling. However, new technologies involving regenerable sulfur sorbents have been devised, and many are proven effective for integrated gasification combined cycle (IGCC) applications [5–9]. These processes remove more than 90% of the sulfur from the hot fuel gas and release it as sulfur dioxide during sorbent regeneration.

The research discussed in this paper investigates use of this sulfur dioxide as a feedstock for synthesis of polymeric ferric sulfate (PFS), a highly effective coagulant used in drinking water and wastewater treatment. PFS is described chemically as $[Fe_2(OH)_n(SO_4)_{(6-n)/2}]_m$, where m is a function of n, $n < 2$ [10,11]. The polymeric (pre-hydrolyzed) nature of PFS offers higher Fe to SO_4 ratios than ferric sulfate, and consumes less alkalinity during its use due to the hydroxyl groups included in the polymeric structure. There is also evidence in the literature that PFS yields a lower rate of floc size development, suggesting a lower rate of formation of hydroxide precipitates and therefore a faster interaction with contaminates in comparison with ferric sulfate [12]. It is effective in removing turbidity, as well as some

* Corresponding author. Tel.: +1-515-294-3951; fax: +1-515-294-3091.
E-mail address: fan@ameslab.gov (M. Fan).

1385-8947/$ – see front matter © 2004 Elsevier B.V. All rights reserved.
doi:10.1016/j.cej.2003.10.007

heavy metal contaminates such as arsenic, at lower temperatures and dosages than other agents.

PFS has been used in place of alum-based agents in some countries, as there are concerns with lifetime cumulative aluminum intake playing a role in the development of neurological disorders such as Alzheimer's disease [13,14]. Meanwhile, preliminary toxicity studies indicate that drinking water treated with PFS is safe for consumption [15]. The potential market for PFS is quite large worldwide, since nearly all municipal water treatment systems using surface water sources rely on a coagulation step in their processes.

Benefits of the process investigated in this research are both environmental and economic. Synthesis proceeds at benign reaction conditions relative to other processes described in the literature [16], thereby reducing construction costs. In addition, no hazardous by-products are released into the environment, ensuring that recurring costs associated with material handling and disposal will be lower as well.

The synthesis system consisted in general of a simple simulated sulfur dioxide gas being sparged into a temperature-controlled reactor containing a solution of ferrous sulfate and water to which an oxidant solution of sodium chlorate was added periodically. The SO_2 absorption and Fe(II) conversion are believed to occur via the pair of reactions given in Eqs. (1) and (2):

$$3SO_2 + ClO_3^- + 3H_2O \rightarrow 3SO_4^{2-} + 6H^+ + Cl^- \quad (1)$$

$$6Fe^{2+} + ClO_3^- + 6H^+ \rightarrow 6Fe^{3+} + 3H_2O + Cl^- \quad (2)$$

where sodium chlorate is used to oxidize the S(IV) to S(VI) and Fe(II) to Fe(III). The iron oxidation is dependent to some extent upon the acid produced in Eq. (1). Water is produced in Eq. (2) and eventually incorporated into the PFS through subsequent hydrolysis, sulfate inclusion, and polymerization as shown in Eqs. (3)–(5).

$$xFe^{3+} + yH_2O \Leftrightarrow Fe_x[(OH)_y]^{(3x-y)+} + yH^+ \quad (3)$$

$$2[Fe_x(OH)_y]^{(3x-y)+} + (3x - y)SO_4^{2-} \Leftrightarrow Fe_{2x}(OH)_{2y}(SO_4)_{(3x-y)} \quad (4)$$

$$m[Fe_{2x}(OH)_{2y}(SO_4)_{(3x-y)}] \Leftrightarrow [Fe_{2x}(OH)_{2y}(SO_4)_{(3x-y)}]_m \quad (5)$$

The PFS structure can also be expressed in a simplified form as $[Fe_2(OH)_n(SO_4)_{(3-n/2)}]_m$, where m is a function of n, and $n = 2y/x$ with $n \leq 2$ [10].

A factorial test was designed to examine the effects of the following four factors on Fe(II) oxidation rate and SO_2 removal efficiency: temperature, SO_2 concentration, nitrogen flow rate, and oxidizer dosing rate. Two levels of each of these four variables were chosen based on what conditions could be produced reliably in the laboratory. Statistical analyses were performed on the SO_2 removal efficiency data using the SAS statistical analysis software (SAS Institute, Cary, NC).

2. Materials and methods

2.1. Equipment

A schematic diagram of the system is shown in Fig. 1. The reaction vessel used was a 4 l jacketed, sealed, glass reaction vessel (Chemglass Inc., Vineland, NJ). A low-temperature silicone oil (Ace Glass Inc., Vineland, NJ) was circulated through the jacket by a heated and refrigerated Neslab RTE-111 temperature bath unit. The reactor's outlet gas stream passed through a condenser, which was maintained at approximately 3 °C by a Cetac model 2050 chiller unit. From there, the sample stream passed through a Permapure model MD-110-48 Nafion concentric tube dryer and then through a Cole-Parmer 0.2 μm in-line particulate filter. Finally, the sample stream entered a California analytical

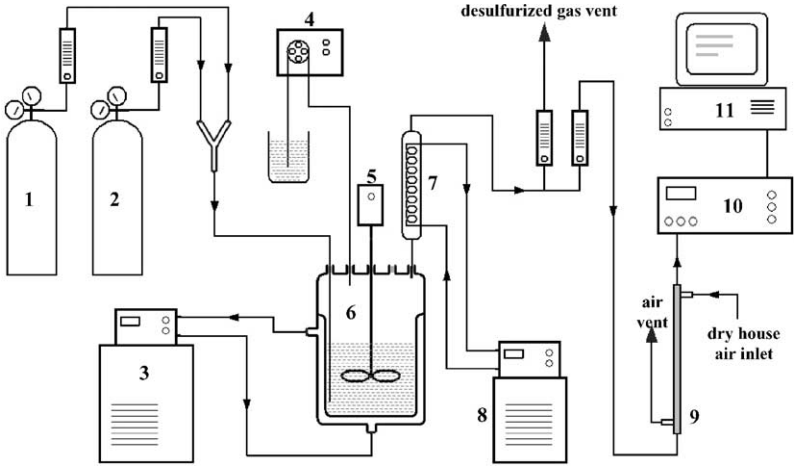

Fig. 1. Schematic of system for PFS synthesis with simulated sulfur gas; (1) nitrogen cylinder; (2) SO_2 cylinder; (3) reactor temperature bath unit; (4) oxidant pump; (5) stirrer motor; (6) jacketed reaction vessel; (7) outlet gas dryer/condenser; (8) condenser chiller unit; (9) Nafion gas dryer tube; (10) SO_2 analyzer; (11) data acquisition computer.

model ZRF NDIR gas analyzer (manufactured by Fuji Electric Company, Saddle Brook, NJ), and then was discharged into the lab fume hood. The gas analyzer reads 0–10% volume SO_2 by 0.01% and has a repeatability of ±0.5% of full scale. It also generates a low-voltage dc signal that was recorded by a desktop computer via a simple data acquisition system.

The reaction mixture was stirred at 200 ± 20 rpm for all trials by an adjustable overhead stirrer connected to a Teflon-coated steel shaft and a Teflon impeller. A Cole-Parmer Masterflex model 7553-50 peristaltic pump added sodium chlorate oxidizer solution through a neoprene drip tube in the top of the reactor at a rate controlled by a ChronTrol model XT digital timer. Mass measurements of the ferrous sulfate, water, and oxidant solution were measured on a Mettler model PM4000 balance having a linearity of ±0.02 g. The gas was sparged into the reactor via an 8 mm glass tube, and reaction temperature was measured with a non-mercury glass thermometer inserted into the reaction mixture. Periodic liquid samples were drawn with an additional 8 mm glass tube temporarily inserted through the top of the reactor. All surfaces in contact with the reaction mixture were either Teflon or glass.

2.2. Reagents

The ferrous sulfate used in the tests was QC Diamond Brand agricultural ferrous sulfate monohydrate (QC Corporation, Cape Girardeau, MO). The sodium chlorate used was Fisher ACS certified sodium chlorate. The sulfur dioxide was anhydrous, 99.98% (Matheson Tri-gas Inc., Montgomeryville, PA). All other reagents used were Fisher ACS certified unless otherwise specified.

The ferrous sulfate was analyzed in the lab for Fe(II) content, and it was found to be 96.5 ± 0.5% pure relative to stoichiometrically pure ferrous sulfate monohydrate. This number was used in the subsequent batch calculations. The oxidant as used in the reaction was a liquid solution of 33.3 wt.% sodium chlorate in distilled water.

2.3. Synthesis procedure

Batches were set up to make 2 kg of liquid PFS with a finished content of 10% iron, and stoichiometric quantities of ferrous sulfate, sodium chlorate, and SO_2 were calculated, and the remaining water required was found by difference. At the start of each run, 630.0 g of ferrous sulfate and 874.5 ± 0.5 g water were added to the reactor. The mass of the container of oxidant solution was also taken before and after the reaction so that the amount consumed could be determined. The calibration of the gas analyzer was verified daily. The span was set using 1.00% SO_2 in nitrogen (BOC Gases, Des Moines, IA) while the zero point was set using dried, filtered house air. This span concentration was thought to be reasonable since the majority of the outlet gas concentrations being measured were less than 2%, and many less than 1%.

After adding the ferrous sulfate and water to the empty reactor, the mixture was stirred for approximately 30 min. before the reaction began to allow the solids to dissolve and the mixture to equilibrate to the temperature of the reactor jacket. At that point, the simulated sulfur gas flow was started, consisting of a blend of SO_2 and nitrogen gases. The gas flow rates were controlled by rotameters, with each inlet concentration being verified by the gas analyzer for use in subsequent removal efficiency calculations. The interval dosing of oxidizer solution was also started with the gas flow. The dosing of oxidizer was set to be one 3 s injection of solution every 1, 2, or 3 min, with each injection containing approximately 0.6 g of sodium chlorate. Details of the reaction conditions are given in Table 1.

Samples were taken from the reactor periodically and analyzed immediately for Fe(II) content. Samples were pulled by opening a port in the reactor lid, inserting a clean glass tube and drawing in a few milliliters of the reaction mixture. Time and temperature were recorded with each sample.

2.4. Analysis of liquid PFS product

Quality parameters for the liquid PFS are well established in the literature [10,16]. The analyses used were total iron, ferrous iron, and basicity (mass ratio of OH/Fe, sometimes referred to as *B* value). Density and pH were also measured.

Table 1
Factorial test conditions for PFS synthesis with midpoints and repetitions

Treatment	Oxidant dose (g/min)	Temperature (°C)	SO_2 concentration (%)	Nitrogen flow (l/min)
1	0.60	39.9	1.9	1.2
2	0.59	41.0	2.2	5.0
3	0.60	42.2	5.4	1.2
4	0.59	43.2	5.3	5.0
5	0.61	61.1	1.9	1.2
6	0.60	60.3	2.2	5.0
7	0.69	63.9	5.4	1.2
8	0.60	60.9	5.3	5.0
9	0.20	34.8	1.9	1.2
10	0.21	34.2	2.2	5.0
11	0.19	35.0	5.4	1.2
12	0.20	34.4	5.3	5.0
13	0.19	57.6	1.9	1.2
14	0.19	54.7	2.2	5.0
15	0.20	57.9	5.4	1.2
16	0.20	54.5	5.3	5.0
Mid1	0.30	47.6	3.7	3.1
Mid2	0.32	47.9	3.7	3.1
Mid3	0.31	47.0	3.7	3.1
Mid4	0.31	47.8	3.7	3.1
Mid5	0.31	47.6	3.7	3.1
R3	0.61	39.0	5.4	1.2
R8	0.62	59.0	5.3	5.0
R12	0.20	34.2	5.3	5.0
R16	0.22	56.4	5.3	5.0

Table 2
PFS quality parameters and optimal value ranges

pH (1 wt.% solution)	2–3
Total Fe (wt.%)	≥9.0
Fe(II) (wt.%)	≤0.1
Density (g/cm^3)	≥1.3
Basicity (wt.%)	8.0–12.0

Table 2 shows the acceptable range of the PFS quality parameters used in this study. Basicity and pH ranges given are based on acceptable behavior of liquid PFS in storage and application. Too high of either value decreases the stability of the product, with a tendency to form precipitates [10]. Meanwhile, a low basicity value indicates a lower degree of polymerization. A very low Fe(II) content is desirable since this species has a tendency to stain fixtures and surfaces and is difficult to precipitate.

The total iron content of the PFS was measured by obtaining a 1.5 g sample of the liquid PFS product and acidifying it with hydrochloric acid. The sample was then heated to boiling, and all iron was reduced to Fe^{2+} by addition of stannous chloride and titanium trichloride. A titration was then performed using a standardized potassium dichromate titrant, with diphenylamine sodium sulfonate indicator. The titration reaction is given here in Eq. (6), and the subsequent calculation of total iron in Eq. (7):

$$6Fe^{2+} + Cr_2O_7{}^{2-} + 14H^+ \rightarrow 6Fe^{3+} + 2Cr^{3-} + 7H_2O \quad (6)$$

$$X_1 = \frac{VC \times 0.05585 \times 6}{M} \times 100\% \quad (7)$$

where X_1 is the total iron concentration (wt.%) in the PFS liquid, V the volume (ml) of potassium dichromate titrant consumed, C the molar concentration of the titrant, M the mass (g) of liquid PFS sample, and 0.05585 is the mass in grams of 0.001 mole of iron.

The concentration of ferrous iron was determined with a similar titration. A sample of approximately 2.0 g of liquid PFS product was acidified with sulfuric and phosphoric acids, and then titrated with a standardized potassium permanganate solution. The net reaction occurring in this analysis is shown in Eq. (8), and the calculation is given in Eq. (9):

$$5Fe^{2+} + MnO_4{}^- + 8H^+ \rightarrow 5Fe^{3+} + Mn^{2+} + 4H_2O \quad (8)$$

$$X_2 = \frac{(V - V_0)C \times 0.05585 \times 5}{M} \times 100\% \quad (9)$$

where X_2 is the ferrous iron concentration (wt.%) in the PFS liquid, V the volume (ml) of potassium permanganate titrant consumed, V_0 the volume (ml) of the titrant consumed by a distilled water blank, C the molar concentration of the titrant, M the mass (g) of liquid PFS sample, and 0.05585 is the mass in grams of 0.001 mole of iron.

The basicity is the mass ratio of OH^- to Fe^{3+} in the polymer, which gives an indication of the degree to which the iron has been hydrolyzed [10,17]. Furthermore, it can be used as a measurement of the extent of polymerization according to the chemical formula for PFS. Basicity was measured by taking a 1.5 g sample of the liquid PFS product and adding to it a known quantity of dilute hydrochloric acid. After allowing the mixture to stabilize for 10 min, a small amount of potassium fluoride was introduced to shield the iron, and phenolphthalein was added as an indicator. The solution was then titrated with dilute sodium hydroxide to find the quantity of acid neutralized by the polymer. The basicity is calculated as shown in Eq. (10)

$$B = \frac{((V - V_0)C \times 0.0170)/17.0}{(M(X_1 - X_2))/18.62} \times 100\% \quad (10)$$

where B is the ratio of OH^- to Fe^{3+} (wt.%), V the volume (ml) of sodium hydroxide titrant consumed, V_0 the volume of the titrant consumed by a distilled water blank, M the mass (g) of liquid PFS sample, C the molar concentration of the titrant, 17.0 the mass (g) of 1 mole of OH^-, 0.017 the mass (g) of 0.001 mole of OH^-, and 18.62 is the mass (g) of 1/3 mole iron.

Density of the liquid PFS product was measured using a 10 ml Gay-Lussac adjusted density bottle (supplied by Cole-Parmer). A direct correlation was found between total iron content and density of the liquid PFS product, allowing a measurement of one of these parameters to be used to estimate the other. pH was measured from a 1.00 wt.% solution of the liquid PFS product in water, using a Corning pH meter 320 calibrated with Fisher certified buffers at pH 1.00 ± 0.02 and pH 4.00 ± 0.02. All titrant solutions and calibrations were made using Fisher ACS certified chemicals and deionized water.

2.5. Characterization of solid PFS

Samples of approximately 2.5 g liquid PFS were dried on standard watch glasses in a Fisher Isotemp model 725G gravity oven. Two samples came from a batch of PFS that was approximately 1 week old, and had an Fe(II) concentration less than 0.1% and a basicity of 10.1%. Both samples were dried for 12 h, one at 60 °C and the other at 90 °C. A third sample, which was dried at 80 °C for 16 h, was also included for comparison. It was taken from a batch of PFS approximately 5 months old, and had an Fe(II) concentration of less than 0.1% and basicity of 7.8%.

After the stated drying period, the samples were removed from the oven and immediately ground vigorously for 3 min with a mortar and pestle. They were then stored in sealed vials until their analysis. The two samples dried for 12 h were stored for approximately 6 weeks before analysis, while the third sample was produced earlier and stored for approximately 10 weeks before its analysis.

The X-ray analyses were carried out using a Philips 1830/00 vertical goniometer and generator unit controlled

by a Philips 1710 APD controller. The X-rays were generated from a copper source operated at 40 kV and 20 mA. Powder samples were placed in a hollow glass slide and scanned from 20 to 120° by 0.2° in the 2θ configuration.

3. Results and discussion

3.1. Stoichiometric model

Examination of the reactions in Eqs. (1)–(5) proposed by Fan et al. [11] gives some insight into the behavior of the basicity quality parameter. In this investigation, basicity of a batch was found to decrease linearly with time if the reaction was continued after the Fe(II) concentration approached zero. This behavior is shown in Fig. 2. At that point the net rate of the reaction in Eq. (2) is near zero, allowing the acid produced in Eq. (1) to accumulate in solution. The decreasing pH causes the reaction in Eq. (3) to slow and eventually reverse, bringing about the reduction in basicity seen in Fig. 2. This is in agreement with the thermodynamic analysis given by Fan et al. [11]. Therefore the amount of time that the SO_2 absorption was continued after all Fe(II) was converted allowed control of this parameter.

The iron measurements made during the course of the synthesis reveal that the initial Fe(II) concentration, equal at that point to the total iron, was greater than 10%. This was due to the fact that as the synthesis progressed, oxidant solution and SO_2 were added to the mixture, decreasing the total iron concentration toward an endpoint target of 10%. However, it was found that the conversion of Fe(II) to Fe(III) was completed before the stoichiometric quantity of SO_2 was added, with some variation depending on the rate of SO_2 absorption and oxidant dosing, as some of the protons required for this reaction were provided by the hydrolysis occurring in Eq. (3). Thus, the synthesis required less SO_2 (and oxidant) than originally calculated. Based on this, the approximate composition of the PFS product solutions, assuming hydrolysis with $n = 2$, was as follows: 50 wt.% PFS (including all dissolved SO_x species), 48 wt.% water, and 2 wt.% sodium chloride.

A mole balance of the reactants is given in Table 3, showing that the rate of SO_2 absorption was 56.0 to 96.1% less than predicted by the reaction stoichiometry in Eqs. (1) and (2) for the Fe(II) conversion rates found. A net accumulation of oxidant was also calculated by taking the oxidant input rate and subtracting the SO_2 absorption and Fe(II) conversion rates divided by their stoichiometric coefficients from Eqs. (1) and (2). It is a small negative quantity in all cases but one, supporting the proposed stoichiometric model if consideration is given to the net storage of SO_2 by the solution saturated with the gas. These calculations assume 10% total iron in the reaction solution, atmospheric pressure in the reactor, and gas flow rates measured at 20 °C.

3.2. Factorial analysis

To obtain trends and statistical results, average SO_2 removal efficiencies were calculated for each run by taking a mean of all the data points starting 30 min after the reaction began and running until the last Fe(II) data point was collected and the reaction was stopped. The initial 30 min period was omitted from the average to allow the outlet gas concentration to stabilize after saturation of the solution and flushing of the headspace in the reactor and tubing. A linear regression was performed on the five Fe(II) concentration values measured during the course of the reaction as well as one initial point calculated from the raw materials added to the reactor to find a concentration versus time slope for each run. This slope was then used to calculate the rate of Fe(II) conversion for each run assuming the batch contained 10% Fe. The R^2 values for the linear fit were above 0.90 in all

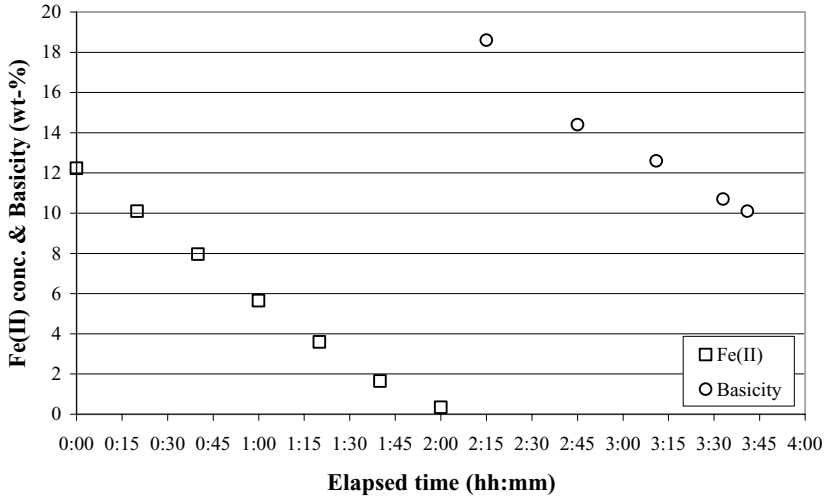

Fig. 2. Decline of basicity after Fe(II) conversion is complete (temperature = 60.4 °C, oxidant dose = 0.61 g/min, SO_2 concentration = 5.4%, nitrogen flow rate = 1.2 l/min).

Table 3
Reactant mole balances showing net oxidant accumulation and stoichiometric ratios

Trial	SO_2 absorption rate[a] (mM/min)	Oxidant input rate (mM/min)	Fe conversion rate (mM/min)	Net oxidant Accumulation[b] (mM/min)	SO_2 deficit[c] (%)
1	0.797	5.634	37.681	−0.912	95.8
2	3.342	5.540	32.122	−0.928	79.2
3	2.321	5.634	34.036	−0.813	86.4
4	5.205	5.540	26.714	−0.647	61.0
5	0.791	5.728	40.327	−1.257	96.1
6	3.067	5.634	35.560	−1.315	82.8
7	2.132	6.479	35.096	−0.081	87.8
8	4.637	5.634	30.088	−0.927	69.2
9	0.761	1.878	10.576	−0.139	85.6
10	1.837	1.972	10.913	−0.459	66.3
11	1.649	1.784	8.302	−0.149	60.3
12	1.653	1.878	7.513	0.075	56.0
13	0.644	1.784	11.876	−0.410	89.1
14	1.412	1.784	10.013	−0.355	71.8
15	1.195	1.878	9.969	−0.182	76.0
16	1.516	1.878	8.566	−0.055	64.6

[a] Rate of SO_2 absorption calculated from concentration and removal efficiency measurements.
[b] Net accumulation of oxidant in the reaction solution.
[c] Percentage less than stoichiometrically predicted quantity of SO_2 absorbed.

cases except one, and greater than 0.95 in most. These two values, average SO_2 removal efficiency and Fe(II) conversion rate, were taken as the quantitative results of each run to be used in the analysis. These values are shown in Table 4.

Due to limitations of the experimental apparatus, the data collected in this study does not allow clear separation of the effects of nitrogen flow rate and SO_2 concentration. Therefore, the SO_2 flow rate as pure SO_2, which is calculated from the nitrogen flow rate and SO_2 concentration, is given with the results in Table 4 and is useful to consider when looking at the behavior of the system.

Prior to undertaking the factorial test, the influence of the gas–liquid mass transfer rate was considered. A series of preliminary experiments showed evidence of a slightly

Table 4
PFS synthesis factorial conditions and results

Treatment	Oxidant dose (g/min)	Temperature (°C)	SO_2 concentration (%)	N_2 flow (l/min)	SO_2 dose (ml/min)	Fe conversion rate[a] (g/h)	SO_2 removal (% of inlet)
1	0.60	39.9	1.9	1.2	22.7	126.2	99.5
2	0.59	41.0	2.2	5.0	114.6	107.5	82.6
3	0.60	42.2	5.4	1.2	68.8	114.0	95.6
4	0.59	43.2	5.3	5.0	277.0	89.4	53.2
5	0.61	61.1	1.9	1.2	22.9	135.0	98.0
6	0.60	60.3	2.2	5.0	114.6	119.1	75.8
7	0.69	63.9	5.4	1.2	68.8	117.5	87.8
8	0.60	60.9	5.3	5.0	277.0	100.7	47.4
9	0.20	34.8	1.9	1.2	22.9	35.4	94.3
10	0.21	34.2	2.2	5.0	114.6	36.5	45.4
11	0.19	35.0	5.4	1.2	68.8	27.8	67.9
12	0.20	34.4	5.3	5.0	277.0	25.2	16.9
13	0.19	57.6	1.9	1.2	22.9	39.8	79.8
14	0.19	54.7	2.2	5.0	114.6	33.5	34.9
15	0.20	57.9	5.4	1.2	68.8	33.4	49.2
16	0.20	54.5	5.3	5.0	277.0	28.7	15.5
Mid	0.30	47.6	3.7	3.1	117.3	51.2	46.9
Mid	0.32	47.9	3.7	3.1	117.3	50.6	50.8
Mid	0.31	47.0	3.7	3.1	117.3	49.9	50.0
Mid	0.31	47.8	3.7	3.1	117.3	52.3	50.2
Mid	0.31	47.6	3.7	3.1	117.3	48.2	51.3
R3	0.61	39.0	5.4	1.2	68.0	123.8	93.0
R8	0.62	59.0	5.3	5.0	277.0	107.1	47.5
R12	0.20	34.2	5.3	5.0	277.0	28.2	24.2
R16	0.22	56.4	5.3	5.0	277.0	31.7	18.0

[a] Fe(II) conversion rate based on a total Fe concentration of 10%.

higher SO_2 removal efficiency (on the order of 10%) with a fine-bubble fritted sparge when compared to an open 8 mm glass tube that released larger bubbles. This difference was ignored in the overall design of the experiment, and the open sparge was chosen for all subsequent tests due to problems with the fritted tubes clogging regularly under the conditions used in the factorial runs. Given the generally high solubility of SO_2 in water, as well as the fact that no quantitative kinetic models were derived from this investigation, the impact of the differences in SO_2 absorption between sparge devices on the results presented here is presumed to be minimal.

Some trends are evident in the data. Foremost it can be seen that the oxidant dosing rate has the most profound effect on both the Fe(II) and SO_2 conversion. In addition, for a given temperature and oxidant dose, SO_2 removal efficiency is inversely proportional to the inlet SO_2 dose due to the oxidant being a limiting reagent. The data also suggest that some temperature effects may be present, which were investigated further and are discussed later in this section.

The statistical analysis for this study was based on 16 factorial runs, and five duplicates of one additional set of conditions near the midpoint of the factorial set. The 16 factorial runs were done in a randomized order, while the midpoints were made as a separate block following. In addition, a repetition of the first four runs was done after the midpoints to examine blocking effects in runs performed after the reactor was replaced due to failure of the drain valve following the final run of the 16 factorial runs. It was determined that blocking effects were not significant between the original and replacement reactors at the 5% level. Analysis of covariance was used to look for evidence of interaction of the reactor with the factors and treatments, and none was found at the 10% level.

Regression models were analyzed to investigate the effects involved between the factors. A model containing blocking, linear, quadratic, and two-way interaction effects (referred to as the full model) was found to give an R^2 value of 0.9852. It is given in Eq. (11), where y is the predicted SO_2 removal efficiency, and the factors oxidant, temperature, sulfur dioxide, and nitrogen are abbreviated by O, T, S, and N, respectively. The terms ρ_1 and ρ_2 are intercepts for each reactor, and β_1–β_4, β_5–β_8, and β_9–β_{14} are coefficients for the linear, quadratic, and two-way cross-product effects, respectively.

$$y = \rho_1 \cdot 1_{(\text{reactor}=1)} + \rho_2 \cdot 1_{(\text{reactor}=2)} + \beta_1 \mathrm{O} + \beta_2 T + \beta_3 \mathrm{S} + \beta_4 \mathrm{N} + \beta_5 \mathrm{O}^2 + \beta_6 T^2 + \beta_7 \mathrm{S}^2 + \beta_8 \mathrm{N}^2 + \beta_9 \mathrm{O}T + \beta_{10} \mathrm{OS} + \beta_{11} \mathrm{ON} + \beta_{12} T\mathrm{S} + \beta_{13} T\mathrm{N} + \beta_{14} \mathrm{SN} \quad (11)$$

This model was compared to a reduced model containing only the blocking and linear effects using a lack-of-fit test. Despite the reduced model having an R^2 value of only 0.9494, it was found that the linear and quadratic terms did not contribute significantly to the full model. The analysis was then reconsidered by treating each of the 17 treatment combinations as classification variables, allowing the data to be analyzed in an ANOVA context (analysis of variance). In this way, the full model can be considered as a subset of the ANOVA model, which had an R^2 value of 0.9978. Another lack-of-fit test performed between the ANOVA model and full model showed that there is still a significant amount of variance that is not explained by the full model, which is likely to lie in three- or four-way interactions between factors.

Table 5
Parameter estimates and statistics for linear regression model

Parameter	Estimate	S.E.	t	$P_r > \lvert t \rvert$
Block 1	61.08	1.72	35.55	<0.0001
Block 2	55.38	2.32	23.91	<0.0001
Oxidant	80.42	7.62	10.55	<0.0001
Temperature	−0.45	0.15	−3.09	0.0060
SO_2	−6.15	0.97	−6.34	<0.0001
N_2	−9.45	0.81	−11.62	<0.0001

Given that the full model is not a significant improvement over the linear model, and that the full model resulted in a saddle point for the optimum factor combination, the results of the regression analysis were taken from the linear model, and are shown in Table 5. The parameter estimates indicate that a high dose of oxidant combined with low values for the other factors resulted in the maximum SO_2 removal efficiency. The absolute magnitude of the t statistic also gives an indication of the relative importance of the factor on the outcome. The fact that nitrogen flow rate appears to be relatively important is related to the effect of the total SO_2 dose, and not expected to be meaningful separately, as discussed above. Both the ANOVA analysis and the linear effects model indicate that maximum SO_2 removal occurs when oxidant concentration is high and the other three factors are low.

3.3. Effect of temperature on synthesis reactions

A series of data runs was performed at different temperatures, with oxidant and gas conditions held constant. SO_2 concentration was set at the 5% level, while nitrogen flow rate was at 1 l/min, and oxidizer was dosed at 1 min intervals. Results are shown in Fig. 3. The rate of Fe(II) conversion increases with temperature, while SO_2 removal efficiency decreases with temperature under the same conditions, most likely due to the faster Fe(II) reaction consuming more of the available oxidant. This effect is visible in runs 9–16 of the factorial tests where the amount of available oxidant is relatively low. This result suggests that the iron reaction is more sensitive to temperature than the SO_2 reaction, such that as the rate of iron conversion increases it consumes more of the oxidant, making less available for the oxidation of SO_2 and thereby reducing its absorption from the gas phase.

3.4. Characterization of solid PFS

The results of the X-ray analysis of the three powder samples produced in the drying trials are shown together in

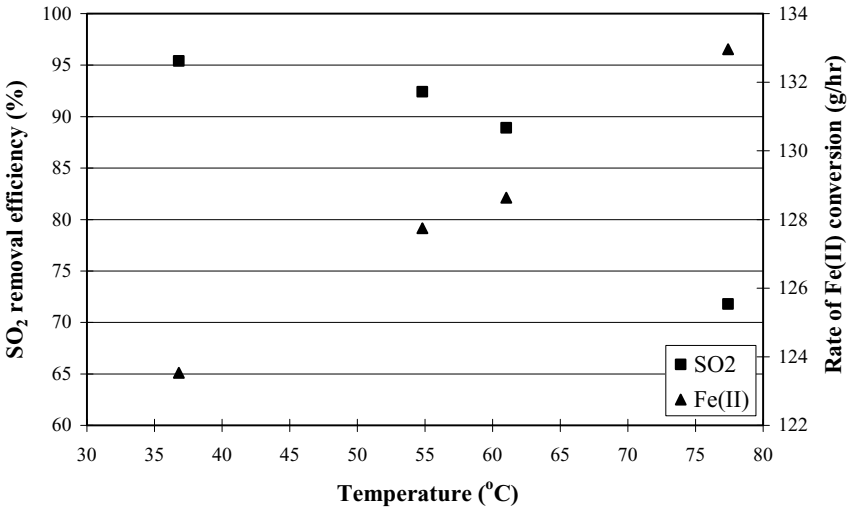

Fig. 3. Effect of temperature on absorption rate of SO_2 and conversion rate of Fe(II) (SO_2 concentration = 5.4%, nitrogen flow rate = 1.2 l/min, oxidant dose = 0.60 g/min as $NaClO_3$).

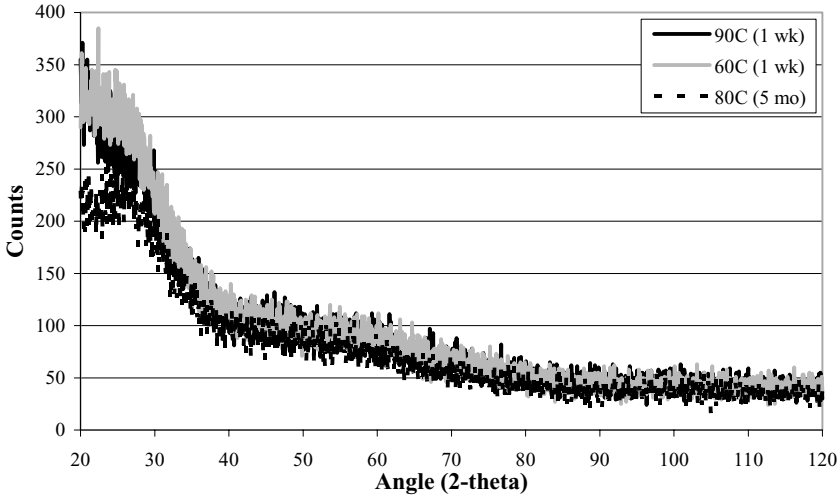

Fig. 4. X-ray diffraction plot from solid PFS produced in the drying trials.

Fig. 4. The absence of any distinct peaks in the diffracted signals suggests that all the dried PFS powder is highly amorphous in nature [18]. A more amorphous solid PFS has been associated with better pollutant removals in bench-scale tests [10]. Very little difference was found between the samples, suggesting that the differences in drying temperature, basicity, and sample age described in Section 2.5 have little or no effect on the crystallinity of the solid PFS.

4. Conclusions

Absorption of sulfur dioxide from a mixed gas stream was investigated by sparging it into a bench-scale reactor containing a stirred solution of ferrous sulfate with sodium chlorate added as an oxidant. The reaction product was a solution containing approximately 50 wt.% polymeric ferric sulfate, a highly effective coagulant useful in treatment of drinking water and wastewater. The reaction took place near atmospheric pressure and at temperatures of 30–80 °C. SO_2 removal efficiencies greater than 90% were achieved with ferrous iron concentrations in the product less than 0.1%.

A factorial analysis of the effect of temperature, oxidant dosage, SO_2 concentration, and gas flow rate on SO_2 removal efficiency suggests that removal efficiency is improved by increasing dosages of oxidant, while it is reduced by an increase in temperature. It is postulated from reaction stoichiometry that the iron reaction is more competitive for the available oxidant at the higher temperatures, which reduced desulfurization efficiency.

The product solution was evaluated by wet chemistry methods to verify that the process was capable of consistently producing high quality PFS. Quality parameters examined were total iron concentration, ferrous iron con-

centration, basicity, density, and pH. It was found that the basicity of PFS could be adjusted by varying how long the absorption and oxidation of SO_2 was continued after all the Fe(II) was converted to Fe(III). In addition, dried, powdered samples of PFS were analyzed by X-ray diffraction to determine whether drying temperature had an effect on relative crystallinities. All samples examined were highly amorphous, suggesting drying conditions had little influence on crystallinity.

References

[1] B.C. Dunn, A. Steinemann, Overcoming the open system problem in local industrial ecological analysis, J. Environ. Plan. Manage. 41 (1998) 661–672.

[2] H. Fan, G. Wu, M. Zhang, Q. Yao, X. Cao, K. Cen, Study on SO_2 removal during pulverized coal combustion, in: Proceedings of the International Conference on Energy and Environment, ICEE, 4–6 May 1998, Shanghai, China, pp. 336–341.

[3] J. Abbasian, A. Rehmat, D. Leppin, D.D. Banerjee, Desulfurization of fuels with calcium-based sorbents, Fuel Process. Technol. 25 (1990) 1–15.

[4] S. Nozawa, I. Morita, T. Mizouchi, Latest SO_x and NO_x removal technologies to answer the various needs of industry, Hitachi Rev. 42 (1993) 43–48.

[5] W. Mojtahedi, K. Salo, J. Abbasian, Desulfurization of hot coal gas in fluidized bed with regenerable zinc titanate adsorbents, Fuel Process. Technol. 37 (1994) 53–65.

[6] R.B. Slimane, J. Abbasian, Copper-based sorbents for coal gas desulfurization at moderate temperatures, Ind. Eng. Chem. Res. 39 (1997) 1338–1344.

[7] R.P. Gupta, W.S. O'Brien, Desulfurization of hot syngas containing hydrogen chloride vapors using zinc titanate sorbents, Ind. Eng. Chem. Res. 39 (1997) 610–619.

[8] Y.X. Li, J. Song, C.H. Li, H.X. Guo, K.C. Xie, A study of high-temperature desulfurization and regeneration using iron-calcium oxides in a fixed-bed reactor, J. Chem. Eng. Chin. Univ. 15 (2001) 133–137.

[9] L. Alonso, J.M. Palacios, R. Moliner, The performance of some ZnO-based regenerable sorbents in hot coal gas desulfurization long-term test using graphite as a pore-modifier additive, Energy Fuels 15 (2001) 1396–1402.

[10] M. Fan, R.C. Brown, S. Sung, C.P. Huang, S. K Ong, J.H. van Leeuwen, Comparison of polymeric and conventional coagulants in arsenic(V) removal, Water Environ. Res. 75 (2003) 308–313.

[11] M. Fan, S. Sung, R.C. Brown, T.D. Wheelock, F. C Laabs, Synthesis, characterization, and coagulation of polymeric ferric sulfate, J. Environ. Eng. 128 (2002) 136–143.

[12] J-Q. Jiang, N.J.D. Graham, Observations of the comparative hydrolysis/precipitation behaviour of polyferric sulphate and ferric sulphate, Water Res. 32 (1998) 930–935.

[13] C.N. Martyn, D.N. Coggan, H. Inskip, R.F. Lacey, W.F. Young, Aluminum concentration in drinking water and risk of Alzheimer's disease, Epidemiology 8 (1997) 281–286.

[14] M. Truchet, Is aluminum a cause of Alzheimer's disease? Can. Med. Assoc. J. 153 (1995) 741.

[15] S. Hendrich, M. Fan, S. Sung, R.C. Brown, L. Semakaleng, R. Myers, G. Osweiler, Toxicity evaluation of polymeric ferric sulfate, Int. J. Environ. Technol. Manage. 1 (2001) 464–471.

[16] Y. Mikami, M. Yanayi, H. Molita, T. Tonaiyama, PPM 5 (1984) 24–32 (in Japanese).

[17] H.X. Tang, W. Stumm, The coagulating behaviors of Fe(III) polymeric species—I, Water Res. 21 (1987) 115–121.

[18] H. Lipson, H. Steeple, Interpretation of X-Ray Powder Diffraction Patterns, Macmillan, London, 1970.